Turkish Journal of Electrical Engineering & Computer Sciences

http://journals.tubitak.gov.tr/elektrik/

Research Article

Turk J Elec Eng & Comp Sci
(2018) 26: 1081 – 1092

doi:10.3906/elk-1704-131

Measurement of active power, electrical energy, and TRMS voltage and current using the dual slope conversion technique

Khaoula KHLIFI*, Amira HADDOUK, Ahlem AYARI, Hfaiedh MECHERGUI
Department of Electrical Engineering, High National School of Engineers of Tunis, University of Tunis, Tunis, Tunisia

Received: 11.04.2017 • **Accepted/Published Online:** 16.01.2018 • **Final Version:** 30.03.2018

Abstract: We have exploited the dual slope (DS) conversion technique to realize an intelligent system with high resolution that ensures active power measurement and electrical energy consumption. The load power is suited by two Hall effect current and voltage transducers, which are associated upstream with a precision analogue multiplier. A DS analogue-to-digital converter (DS-ADC) performs the conversion by rejecting noise with a conversion time that is multiple frequencies of the ADC's first slope. The digital acquisition is made by a PIC 16F877 using a management algorithm ensuring the control, acquisition, and treatment of information. Results are displayed on a 2-line and 16-column LCD. The developed instrument is programmable, which gives it many advantages, such as speed of execution, measurement reliability, and error correction.

Key words: DS-ADC, nonlinear load, harmonics rejection, treatment by PIC, electrical energy

1. Introduction

Nowadays, new technology includes a lot of home equipment that is more sensitive to load power, such as computers and electronic devices containing different kinds of power. It results in a deterioration of power quality in distribution and affects the performances of this electric equipment. Therefore, an impact of the expenses of customer invoice is needed, which necessitates measuring the true energy consumed [1–4].

Most of the developed techniques for measuring energy are theoretical and are insufficient in detailed description [2,3].

Intelligent measurement systems contribute to optimizing maintenance, controlling the electrical energy quality, and protecting the installations. This paper presents an interesting method using a dual-slope analogue-to-digital converter (DS-ADC) with high resolution to measure the RMS value of the current, voltage, active power, and energy for linear and nonlinear loads. We use quasisynchronous sampling with the first harmonic of the voltage network. This method eliminates the discretization error and harmonics that are not isochronous and it has high noise immunity [5].

This technique extracts the resulting true power of the product of isochronous currents and voltage harmonics. The developed system is in fact a contribution to the realization of a high-resolution intelligent measurement instrument. The prospects are directed towards energy management in smart houses and it is simple in design [6].

*Correspondence: khlifi.kh@hotmail.com

2. Proposed work

A functional block diagram of the energy meter prototype is shown in Figure 1. This system is designed based on a PIC microcontroller, which acts as a data processing and transmission system.

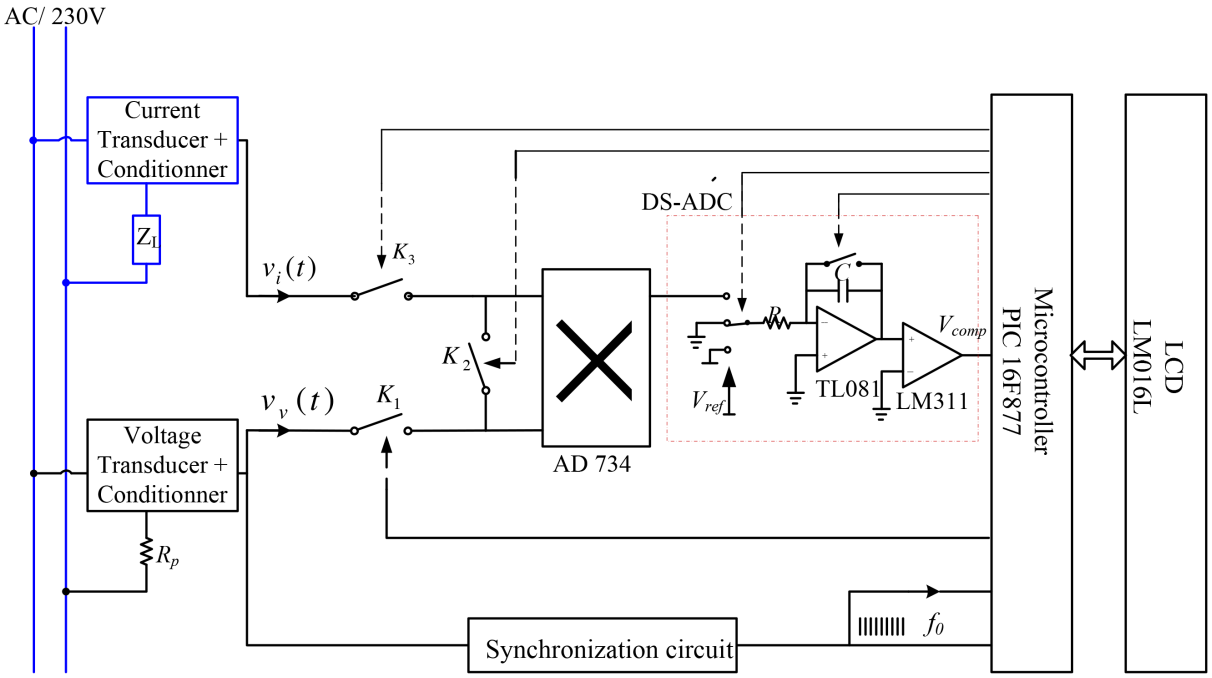

Figure 1. Block diagram of the measurement system.

The voltage line and the current load are obtained using voltage Hall effect transducers LV-25P and current Hall effect transducers LEM LA25-NP, respectively. They are used to adapt the measuring power and also to assure a galvanic insulation. Indeed, the signal at the output of a sensor is generally weak and it is necessary to amplify it and condition it. An analogue multiplier device (model AD734) was used to measure power, which assured the multiplication of the two conditioners. The output signal of this is applied to the input of a DS-ADC. Digital information of the output of the DS-ADC is processed by a PIC 16F877 microcontroller, which is followed by an LCD display.

According to Figure 1, the switches K_1, K_2, and K_3 are used to obtain the effective value of the current, the voltage, and the power.

3. Calculate the power and energy using the DS-ADC

In a general case, the adaptation of a sensor with an analogue output voltage to a system of digital instrumentation via an ADC causes large systematic errors, especially when the difference between the two periods is very low. The ADC accepts the element directly from an input sensor and provides a digital output proportional to the physical quantity being read by the latter. We turn, then, towards more compact and more robust converters. Consequently, the complexity decreases, which leads us to error reduction and increased reliability. The DS-ADC needs only two integration times and it is one way of integrating ADCs, providing high resolution and high noise rejection [5,7]. It can be found in many applications for digitizing low-bandwidth signals, such as digital multimeters and panel meters, which require no high-speed operations. The voltage and current

waveforms of the power network, however, are not strictly periodic, due to their lack of harmonic components and stochastic variation.

The measurement method described in this work can be applied for measuring active power and consumed energy. The synchronous method is based on DS integration performed according to the synchronization signal of the network voltage. The DS-ADC procedure for the measurement of power is illustrated in Figure 2. Analysis of this schema, which forms the basis of the designed measurement system, highlights the rejection of undesirable waves during the conversion [8].

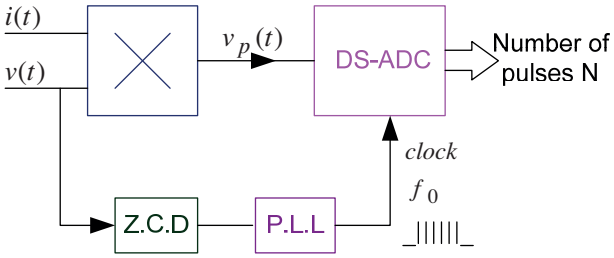

Figure 2. Block diagram of the power measurement using DS-ADC.

The first phase of integration is entirely synchronized with the input signal and its duration is also measured. The output voltage integrator depends directly on the input signal and the time of the first phase of integration. Figure 3 shows the operation cycle of the ADC, where T_m is set and t_x is measured. We exploit the phase-locked loop (PLL) technique to develop the real-time clock of the DS-ADC: the measurement signals are synchronized to the network frequency. Indeed, a PLL realizes the elaboration of the clock to pilot the ADC. The clock frequency is a multiple of the network frequency.

We have

$$T_m = k\,T_r \tag{1}$$

Thus,

$$T_r = M_n\,T_0 \tag{2}$$

Substituting Eq. (1) in Eq. (2) results in

$$T_m = k\,M_n\,T_0 \tag{3}$$

Otherwise, we have

$$T_m = M\,T_0 \tag{4}$$

Using Eqs. (3) and (4), we obtain

$$k = \frac{M}{M_n} \quad (k : Constant), \tag{5}$$

where

T_m: The time of the first integration slope.

T_r: The period of electrical network.

T_0: The clock period.

M: Number of impulses counted during the time T_m.

T_0 is no longer in Eq. (5) and so the sampling error is eliminated. Indeed, with this method, we have solved the problem of the discretization error and whatever changes in the grid period T_r, the time T_m of the first slope is synchronized and is a multiple of the grid frequency. Thus the ratio is constant.

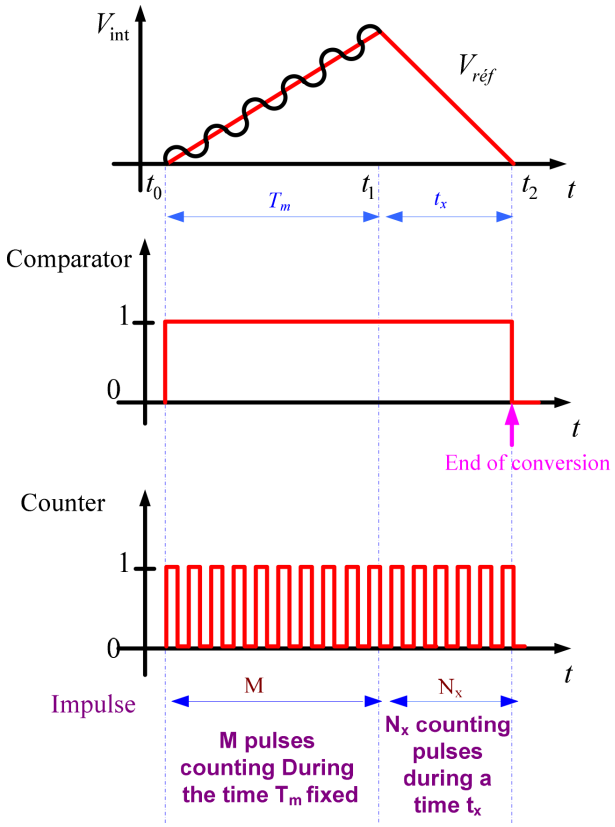

Figure 3. The operation cycle of the DS-ADC.

The analytical operation principle of the DS-ADC is as follows:

- The first slope : $0 \leq \quad t \quad \leq \quad T_m$

At the output of the integrator we have

$$V_{DS-ADC_1} = -\frac{1}{RC}\int_0^{T_m} v_x(t)\,dt \tag{6}$$

- The second slope: $t_1 \leq \quad t \leq t_2$ or $0 \leq t \leq t_x$

At the output of the integrator, the voltage V_{DS-ADC_2} can be written as follows:

$$V_{DS-ADC_2} = -\frac{1}{RC}\int_0^{t_x} V_{ref}\,dt + V_{DS-ADC_1}, \tag{7}$$

where V_{ref} is the reference voltage.

At $t = t_x$, we have

$$V_{DS-ADC_2} = -\frac{V_{ref}}{RC}\ t_x + V_{DS-ADC_1} = 0 \tag{8}$$

Hence,

$$\frac{V_{ref}}{RC}t_x = \frac{1}{RC}\int_0^{T_m} v_x(t)\,dt \tag{9}$$

Substituting the values of Eq. (4) and $t_x = N_x T_0$ into Eq. (9) we obtain

$$v_x = \frac{V_{ref}}{M}N_x, \tag{10}$$

where
N_x: the number of impulses counted during the time t_x.

Using Eq. (10) and according to Figure 1, we can measure V_{RMS}, I_{RMS}, and the active power P:

$$\text{With: } \begin{cases} v_i(t) = G_i\,K_{Hi}\,I_m \sin(\omega t + \varphi) \\ v_v(t) = G_v\,K_{Hv}\,R_m\,V_m \sin(\omega t) \end{cases} \tag{11}$$

i. If we close the switches K_1 and K_2 at the output of the multiplier we obtain the effective value of the voltage, as shown in Figure 4.

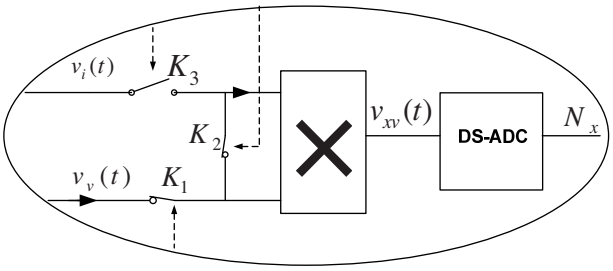

Figure 4. Modeling of the measurement system of V_{RMS}, I_{RMS}, and P.

$$v_{xv}(t) = v_v^2(t) = G_v^2\,k_{Hv}^2\,k_X\,[V_m \sin(\omega t)]^2 \tag{12}$$

$$v_{xv}(t) = k_v\,V_m^2\left(\frac{1-\cos 2\omega t}{2}\right), \tag{13}$$

where
G_v: Gain of the voltage conditioner.
k_{Hv}: Scaling factor of the voltage Hall effect sensor.
k_X: Multiplier constant.

$$k_v = G_v^2\,k_{Hv}^2\,k_X$$

Thus, during the first slope of integration, we have

$$V_{DS-ADC_1} = -\frac{1}{RC}\int_0^{T_m} v_{xv}(t)\,dt \tag{14}$$

After calculation using Eqs. (7), (8), and (10), we have

$$\frac{V_m^2}{2} = \frac{V_{ref}}{M \cdot k_v} N_x \tag{15}$$

From Eq. (15), we obtain the RMS value of the network voltage:

$$V_{eff}^2 = k_{t1}\, N_x, \tag{16}$$

where $k_{t1} = \frac{V_{ref}}{M.\, k_v}$

ii. Using Figure 4, if we close the switches K_2 and K_3 at the output of the multiplier we can have the effective value of the current:

$$v_{xi}(t) = v_i^2(t) = G_i^2\, k_{Hi}^2\, R_m^2\, k_X \left[I_m^2 \sin^2(\omega t + \varphi)\right] \tag{17}$$

$$v_{xi}(t) = k_i\, I_m^2 \left(\frac{1 - \cos\left(2\omega t + 2\varphi\right)}{2}\right) \tag{18}$$

with:
G_i: Gain of current conditioner.
k_{Hi}: Scaling factor of the current Hall effect sensor.
R_m: Current shunt resistor.

$$k_i = G_i^2\, k_{Hi}^2\, R_m^2\, k_X$$

During the first slope of integration, we have

$$V_{DS-ADC_1} = -\frac{1}{RC} \int_0^{T_m} v_{xi}(t)\, dt \tag{19}$$

After calculation using Eqs. (7), (8), and (10), we have

$$\frac{I_m^2}{2} = \frac{V_{ref}}{M \cdot k_i} N_x \tag{20}$$

From Eq. (20), we obtain, at the output of the DS-ADC, the RMS value of the network current:

$$I_{eff}^2 = k_{t2}\, N_x, \tag{21}$$

where $k_{t2} = \frac{V_{ref}}{M.\, k_i}$

iii. According to Figure 4, if we close the switches K_1 and K_3 at the output of the multiplier we can have the power P:

$$v_{xy}(t) = k_x\, v_i(t)\, v_v(t) \tag{22}$$

$$v_x(t) = G_v\, k_{Hv}\, G_i\, k_{Hi}\, R_m\, k_X \left[V_m \sin\left(\omega t\right) \times I_m \sin\left(\omega t - \varphi\right)\right] \tag{23}$$

We put $v_{xy}(t) = v_p(t)$

$$v_p(t) = k_p V_m I_m \left[\frac{\cos\varphi - \cos(2\omega t + \varphi)}{2}\right], \tag{24}$$

where k_p is noted the power which is written as follows: $k_p = G_v k_{Hv} G_i k_{Hi} R_m k_X$.

During the first slope of integration, we have

$$V_{DS-ADC_1} = -\frac{1}{RC}\int_0^{T_m} v_p(t)\,dt \tag{25}$$

After calculation using Eqs. (7), (8), and (10), we have

$$V_{RMS} I_{RMS} \cos\varphi = \frac{V_{ref}}{M \cdot k_p} N_x \tag{26}$$

From Eq. (26), we obtain, at the output of the DS-ADC, the active power:

$$P = k_{t3} N_x, \tag{27}$$

where $k_{t3} = \frac{V_{ref}}{M \cdot k_p}$

From Eq. (27), we note that the active power is proportional to N_x.

If the load is nonlinear, we have

$$\begin{cases} v(t) = V_{1m}\sin(\omega t) + V_{3m}\sin(3\omega t) + V_{5m}\sin(5\omega t) + \cdots \\ i(t) = I_{1m}\sin(\omega t + \phi_1) + I_{3m}\sin(3\omega t + \phi_3) + I_{5m}\sin(5\omega t + \phi_5) + \cdots \end{cases} \tag{28}$$

The signal $v_p(t)$ is then applied to the DS-ADC. There, we take back the two main phases:

- The first slope : $0 \leq t \leq T_m$

$$V_{DS-ADC_1} = -\frac{1}{RC}\int_0^{T_m} v_p(t)\,dt \tag{29}$$

$$V_{DS-ADC_1} = -\frac{k_p}{RC}\int_0^{T_m}\begin{bmatrix} \frac{V_{1m}\,I_{1m}}{2}\left[\cos\phi_1 - \cos\left(2\omega t+\phi_1\right)\right]dt \\ \frac{V_{1m}\,I_{3m}}{2}\left[\cos\left(2\omega t+\phi_3\right) - \cos\left(4\omega t+\phi_3\right)\right]dt \\ \frac{V_{1m}\,I_{5m}}{2}\left[\cos\left(4\omega t+\phi_5\right) - \cos\left(6\omega t+\phi_5\right)\right]dt \\ \frac{V_{3m}\,I_{1m}}{2}\left[\cos\left(2\omega t-\phi_1\right) - \cos\left(4\omega t+\phi_1\right)\right]dt \\ \frac{V_{3m}\,I_{3m}}{2}\left[\cos\phi_3 - \cos\left(6\omega t+\phi_3\right)\right]dt \\ \frac{V_{3m}\,I_{5m}}{2}\left[\cos\left(2\omega t-\phi_5\right) - \cos\left(8\omega t+\phi_5\right)\right]dt \\ \frac{V_{5m}\,I_{1m}}{2}\left[\cos\left(4\omega t-\phi_1\right) - \cos\left(6\omega t+\phi_1\right)\right]dt \\ \frac{V_{5m}\,I_{3m}}{2}\left[\cos\left(2\omega t-\phi_3\right) - \cos\left(8\omega t+\phi_3\right)\right]dt \\ \frac{V_{5m}\,I_{5m}}{2}\left[\cos\phi_5 - \cos\left(10\omega t+\phi_5\right)\right]dt \end{bmatrix} \tag{30}$$

It is noted that Eq. (30) can be decomposed into two terms, which are, respectively, the DC and AC component of the power.

When selecting T_m multiple of the network period, the AC components will be rejected. Then for the first slope we have

$$V_{DS-ADC_1} = -\frac{k_p}{RC}T_m\left(\frac{V_{1m}\,I_{1m}}{2}\cos\phi_1 + \frac{V_{3m}\,I_{3m}}{2}\cos\phi_3 + \frac{V_{5m}\,I_{5m}}{2}\cos\phi_5\right) \tag{31}$$

The synchronization is adapted using the PLL.

- The second slope : $t_1 \le t \le t_2$ or $0 \le t \le t_x$

$$V_{DS-ADC_2} = -\frac{V_{ref}}{RC}t_x + V_{DS-ADC_1} = 0 \tag{32}$$

The substitution of Eq. (31) into Eq. (32) gives

$$k_p\left(\frac{V_{1m}\,I_{1m}}{2}\cos\phi_1 + \frac{V_{3m}\,I_{3m}}{2}\cos\phi_3 + \frac{V_{5m}\,I_{5m}}{2}\cos\phi_5\right) = -\frac{V_{ref}}{T_m}t_x \tag{33}$$

Or in absolute value

$$k_p\left(V_{eff1}\,I_{eff1}\cos\phi_1 + V_{eff3}\,I_{eff3}\cos\phi_3 + V_{eff5}\,I_{eff5}\cos\phi_5\right) = \frac{V_{ref}.t_x}{T_m} \tag{34}$$

thus,

$$k_p\left(V_{eff1}\,I_{eff1}\cos\phi_1 + V_{eff3}\,I_{eff3}\cos\phi_3 + V_{eff5}\,I_{eff5}\cos\phi_5\right) = \frac{V_{ref}}{M}N_x \tag{35}$$

Consequently, the power is

$$P = \sum P_i = \frac{V_{ref}}{M\cdot k_p}N_x \tag{36}$$

If we set $h = \frac{V_{ref}}{M \cdot k_p}$ the measured power is given by the following equation:

$$P = h \times N_x \tag{37}$$

This technique is based on the use of a DS-ADC with a selected resolution of 20,000 measurement points, which gives a high resolution. By counting the number of pulses N_x, we can directly deduct the power P. The consumed energy is then calculated based on the active power value for each frame of 1 s, which means

$$W_e = P \times \Delta t(\text{During1}s) \tag{38}$$

The DS-ADC can be well exploited to measure power and any load because it constitutes a rejecter of harmonics having a multiple period of the first integration. The method using the DS conversion technique also performs the measurement of V_{eff} and I_{eff}.

4. The smart energy meter implementation

4.1. Management algorithm

The measuring system using DS-ADC is built around a microcontroller PIC 16F877. It is a low-cost microcontroller that has 8 analogue inputs. The microcontroller is programmed to calculate the active power (for linear or nonlinear loads) and the energy and to display them on the LCD. Figure 5 shows the measurement flow chart used to indicate the processing algorithm for the management and acquisition of the magnitudes and experiment process.

4.2. Electronic design of the energy meter

The realized electronic circuit for conditioning voltage and current is shown in Figure 6a. The product result is thereafter done by the analogue multiplier. Figure 6b depicts the electronic diagram relative to DS-ADC and the PLL. Finally, in Figure 6c, we have the digital processing, which is composed by a microcontroller, followed downstream by the LCD.

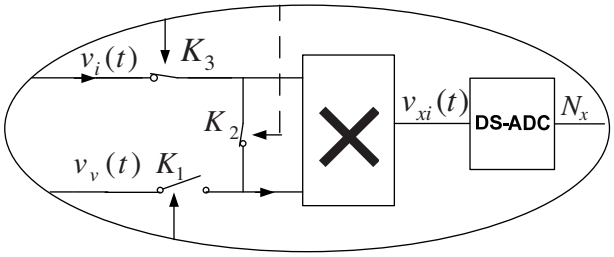

Figure 5. Measurement algorithm management.

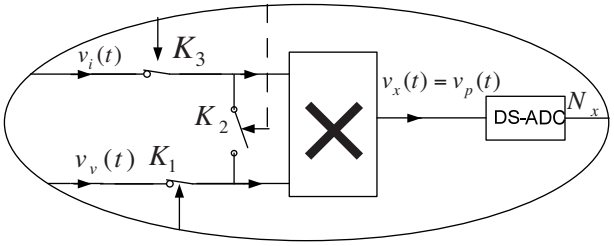

Figure 6. Electronic diagrams of the energy meter.

4.3. Hardware implementation

The hardware design of the energy meter using DS-ADC, presented in Figures 7 and 8, has been implemented and tested.

5. Metrological analysis and sources of errors associated with the energy meter

To evaluate the measurement error, Eqs. (10) and (36) are used, which constitute the conversion function of the DS-ADC.

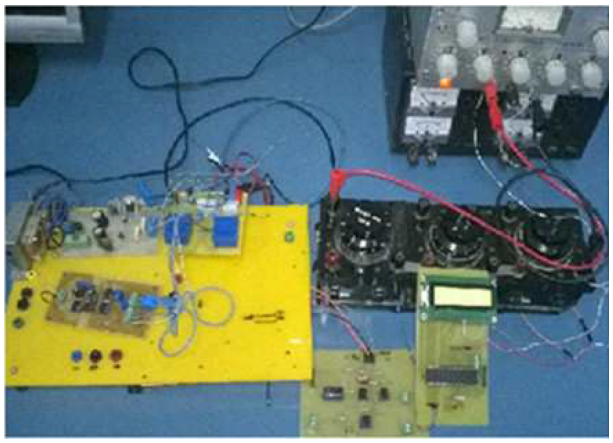

Figure 7. Instrumental platform representing the energy meter.

Figure 8. The active power and the energy values measured by PIC 16F877.

$$\text{If } Nmax = M = 20000 = 2^n \rightarrow nbits \tag{39}$$

Eq. (10) can be written as

$$P = \frac{1}{k_P} \times \frac{V_{ref}}{2^n} N_x = \frac{1}{k_P} \times \frac{V_{ref}}{2^n} \sum_{i=0}^{n-1} a_i 2^i, \tag{40}$$

where $a = \begin{cases} 0 \\ \text{or} \\ 1 \end{cases}$

The measuring system can be modeled as shown in Figure 9 [9].

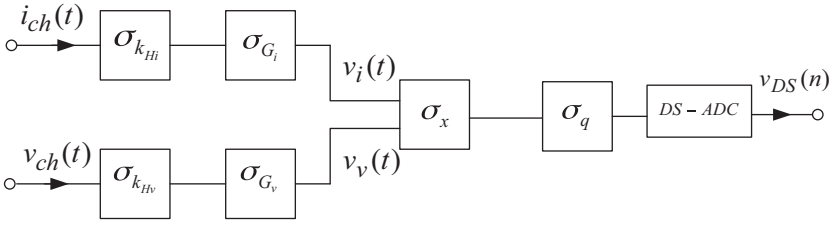

Figure 9. Metrological modeled diagram of the energy meter system.

The DS-ADC performs N_x samples of the signal at the output of the multiplier and introduces a noise due to the quantization, which is represented in Figure 10.

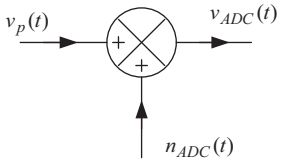

Figure 10. Modeling of the DS-ADC.

We used a DS-ADC of 15 bits with a reference DC voltage of 2 V. The quantum (q) of the DS-ADC is

$$q = \frac{V_{réf}}{2^{15}} = \frac{2}{32768} = 0.061\,[mV] \tag{41}$$

The parameters involved in Eq. (40) are independent. Then we use an error propagation method.

$$\sigma p = \sqrt{\left(\frac{\partial p}{\partial q}\right)^2 (\sigma q)^2 + \left(\frac{\partial p}{\partial k_p}\right)^2 (\sigma k_p)^2} \tag{42}$$

From Eq. (42), which gives the variance of the error, we determine the uncertainty error due to the measurement system:

$$\frac{\sigma_p}{p} = \sqrt{\left(\frac{\sigma q}{q}\right)^2 + \left(\frac{\sigma k_{Hv}}{k_{Hv}}\right)^2 + \left(\frac{\sigma k_{Hi}}{k_{Hi}}\right)^2 + \left(\frac{\sigma G_v}{G_v}\right)^2 + \left(\frac{\sigma G_i}{G_i}\right)^2 + \left(\frac{\sigma k_x}{k_x}\right)^2 + \left(\frac{\sigma R_m}{R_m}\right)^2} \tag{43}$$

$$\frac{\sigma_p}{p}(\%) = \sqrt{\sum \left(\frac{\sigma x_i}{x_i}\right)^2} \times 100 \tag{44}$$

A sensor with an accuracy of 0.1% and conditioner elements with an accuracy of 0.2% are selected.

After all calculations using an autocalibration system and each early data acquisition operation, the error can be less than 0.2% for a voltage range of 230 V and a current range of 10 A.

6. Conclusion

A DS-ADC method for energy measurement has been presented in this work. The solution described is used for the measurement of the TRMS of the voltage and the current, the active power, and energy for a linear or nonlinear load. The synchronization of the ADC first slope with the network frequency removes the discretization error. The developed instrument using a DS-ADC allows us to measure also the reactive power and the deformation factor.

All the system can be connected via a wifi transmitter to send the data information to a measurement station managed by PC. The developed instrument is programmable, which gives it many advantages, such as speed of execution, measurement reliability, and error correction.

This instrument represents a smart energy meter using a new simple technique with high resolution.

References

[1] Vanya I. Méthodes d'analyse de la qualité de l'énergie électrique: application aux creux de tension et à la pollution harmonique. Thesis, Université Joseph Fourier. Grenoble, France, 2006.

[2] Thousif A, Sreedevi A. Design and development of pic microcontroller based 3 phase energy meter. International Journal of Innovative Research in Science, Engineering and Technology 2014; 3: 1370-1379.

[3] Bhaskar S, Sreenivasulu S, Polaiah B. Intelligent system for single phase energy meter billing and action taking using wireless network. International Journal of Advanced Information and Communication Technology 2014; 1: 2348-9928.

[4] Sapna G, Pravesh G. Prepaid energy meter for billing system using microcontroller and recharge card. International Journal of Core Engineering and Management 2014; 1: 2348-9510.

[5] Astuo M, Shuichi N. Noise immunity characteristics of dual-slope integrating analog-digital converters. In: 1999 International Symposium on Electromagnetic Compatibility; 17–21 May 1999; Tokyo, Japan; IEEE. pp. 622-625.

[6] Mohan NM, George B, Kumar VJ. A novel dual-slope resistance-to-digital converter. IEEE T Instrum Meas, 2010; 5: 1013-1018.

[7] Hasan K. A dual-slope integration based analog-to-digital converter. American Journal of Engineering and Applied Sciences 2009; 4: 743-749.

[8] Daugherty KM. Analog to Digital Conversion: A Practical Approach. New York, NY, USA: McGraw-Hill, 1995.

[9] Haddouk A, Mechergui H, Ayari A. Instrumental platform controlled by Labview for the power measurement and electric circuits characterisation. In: 8th International Multi-Conference on Systems, Signals and Devices (SSD); 22–25 March 2011; Sousse, Tunisia. In: IEEE Xplore, 2011.